Technical Article

Electromagnetic Optimal Design of a Permanent Magnet Synchronous Generator.

Abstract —**This article presents an optimal design of a Permanent Magnet Synchronous Generator (PMSG). A comprehensive correlation analysis is presented to determine a reduced subset of design variables that makes faster the PMSG design. Such design is achieved by representing a cost function with two Kriging metamodels and using the Latin Hypercube sampling method. The first Kriging represents the generator's weight, whereas the second one represents the generated electrical power. Both Kriging models were developed using 3D-FE time-stepping PMSG simulations. The resulting multiobjective problem was solved with a global genetic optimizer.**

I. Introduction

Several decades ago, the design of electrical machines was based on theoretical designs, and small prototypes were fabricated for validation. Currently, powerful computers, accurate three-dimensional electromagnetic models, statistics, design of experiments, and mathematical programming allow reducing the cost and design time [1]. Nevertheless, it is well-known the difficult to develop detailed numerical models and obtain the optimal design of electrical machines due to the large number of variables that define their performance [2]. Finite Element (FE) models are accurate, but their direct use in the design optimization of electromagnetic devices demands high computational time. Hence, the usage of design of experiments and surrogate modelling like Kriging and response surface models to represent complex electromagnetic systems have successfully been used [3]-[5]. Alternatively, simplified physics-based models based on analytical relationships and magnetic reluctance networks combined with FE models and global optimization methods have been successfully used to find more accurate machine designs [6]. Furthermore, multiobjective global optimizers such as swarm and genetic algorithms have also been applied to the design of electromagnetic devices [7]- [9].

The design of electrical machines is important for any type of their application. In the basic design of a machine, specific procedures and analytical strategies must be considered to carry out the calculation of the magnetic circuit, electrical circuit, efficiency, type of insulation, number of poles and slots, dimensions of the winding, demagnetization, analysis of cogging torque, noise, vibration, torque ripple, speed range, torque density, control strategies, use of materials, cost of products, structural and thermal design, and manufacturing techniques [10]. In the solution of the above design problems, mathematical models are required, which are generally based on the Finite Element Method (FEM). In the search for optimal performance, multiobjective or single-objective optimization methods are used. In recent years global optimization methods based on evolutionary algorithms have played a significant role [11]-[13]. Genetic algorithms and the metamodel based on the Kriging algorithm have successfully been used to find the optimal design of motors used in compressors, where the shape of the rotor is optimized to improve the cogging torque [14]. On the other hand, the use of a sleeve has been investigated to reliably fixate the permanent magnets and prevent their detachment due to centrifugal forces. The sleeve must have low eddy current losses for avoiding heating and demagnetization of the permanent magnets. This design can be achieved by using 2D and 3D Finite Element (FE) models in conjunction with response surface models [15], [16]. Torque ripple reduction has been one of the primary considerations in the optimal design of synchronous reluctance machines. Various techniques have been employed, including optimal slot/pole ratio, stator slot skewing, rotor magnet skewing, and pole face optimization [17]. Hu and Wang used the third harmonic method to optimize the pole faces of surface permanent magnets and demonstrated the increase in the average electromagnetic torque [18]. In reference [19], Wang et al. investigated the optimization of the vibration of a permanent magnet motor. They used the weighted method of the particle accumulation optimizer by adjusting the coefficient of the polar arc, the thickness of the permanent magnet, and the width of the stator slot and stator slot opening. In reference [20], the authors reported the use of reluctance networks to investigate the optimal number of poles in an electric machine of a hybrid vehicle. S. Fang et al. [21] published the results of electromagnetic torque ripple optimization in a permanent magnet motor and reported a decrease in torque ripple from 31.7% to 1.17%. In reference [22], the air gap shape optimization was presented to minimize the air gap ripple in permanent magnet synchronous motors. They used a search optimization method based on mesh on/off. The air gap is the parameter that most correlates with the machine's behaviour, where changes in the shape of the flux density cause substantial changes in the distribution of forces. Likewise, the behaviour of motors with concentrated fractional windings have been investigated considering different combinations of slots/poles; the FEM was also used for electromagnetic and acoustic analysis [23], [24]. In reference [25], the topological optimization of permanent magnet machines is presented. In reference [26] vibrations in internal permanent magnet motors were analyzed where the deformation of the air gap was considered. The FEM was also used to calculate the radial force density in the rotor.

This article presents the optimization of a PMSG design, where a correlation and sensitivity analysis, the electrical machine modeling for design purposes, and an optimization algorithm are used. The application of correlation and sensitivity analysis allows finding a reduced design space with the most significant design variables. By using Kriging theory, two metamodels are developed to represent the PMSG electrical output power and the material weight of the PMSG. The resulting cost function is solved by employing multiobjective genetic algorithms.

II. PMSM modeling for optimization

In developing the optimal design of an electromagnetic device, all possible interactions of the processes or variables involved in its operation must be considered. That is, all the physical variables that are part of the process must be taken into account. For example, a low-frequency electric motor is commonly controlled by an electronic system. Additionally, the motor is designed to produce mechanical output. The interaction with the electronic system and the interaction with the mechanical

system must be considered in the machine design. Any attempt to optimize one or more variables of this electrical machine must consider all the related components. This implies a problem of greater complexity since it is necessary to investigate areas other than traditional electromagnetic analysis. In other words, the number of variables increases considerably, which complicates obtaining the optimal model of the electrical machine. Nowadays, the designer performs the optimization of a device using a computer-aided design tool. Nevertheless, even when the advantages in computational resources are powerful, numerical models of electromagnetic devices, such as those developed with design tools based on the FEM, cannot provide the interactions between the variables involved with the objectives to be optimized.

A. The proposed optimal design approach

The proposed approach can be seen in Fig. 1, where it starts with the initial geometry of the generator. Then, a statistical analysis is made to obtain the correlation and sensitivity of the design variables with the objective functions [27]. This allows determining a reduced design space since there are many design variables in an electrical machine. Nevertheless, not all of them have a substantial impact on the cost functions. If a reduced set of design variables can be found, then a faster design can be achieved. The next step is to apply a design of experiments that, in this case, Latin Hypercube and 3D-FE time-stepping simulations were used to determine the generator's performance. With this data, a Kriging model is built from both the design variables and the output response. The next step is to execute the multiobjective optimization, where a second-generation evolutionary genetic algorithm is applied. The output of this optimizer is a set of feasible and optimal solutions.

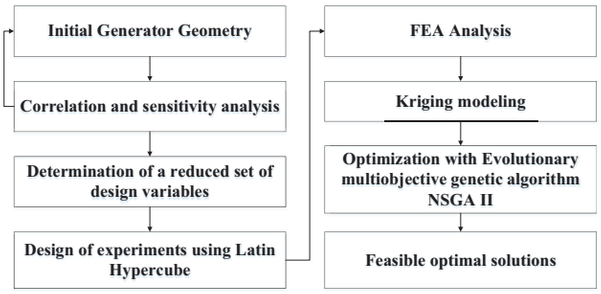

Fig. 1 Proposed optimal PMSG design methodology.

B. Machine sizing

The conventional sizing procedure is illustrated in Fig. 2. The first step in designing a generator is to define the power, voltage, speed, and type of the winding connection. With this data, it is then possible to calculate the main dimensions and the length of the airgap. Subsequently, the types of windings must be selected, that is, if it is one-layer, two-layers, distributed, or a concentrated winding. With this data and using an approximation of the airgap flux density, the number of winding turns and the current density allowed in the windings can be calculated. Hence the information of the number of conductors and their diameter is determined. In the next step, the dimension of the stator slots, and where the conductors are located, is determined. This data makes it possible to calculate the flux density in the airgap, in the stator, and the rotor. Next, the inside and outside diameters of the rotor and stator as well as the axial length are calculated. The resulting PMSG geometry is shown in Fig. 3. Finally, with all the geometry data, it is possible to compute the performance of the electric machine.

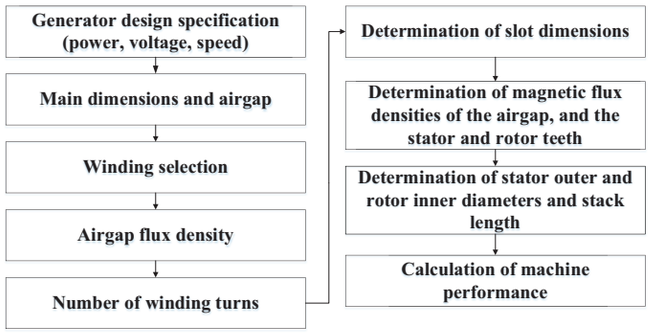

Fig. 2. Sizing of a PMSG.

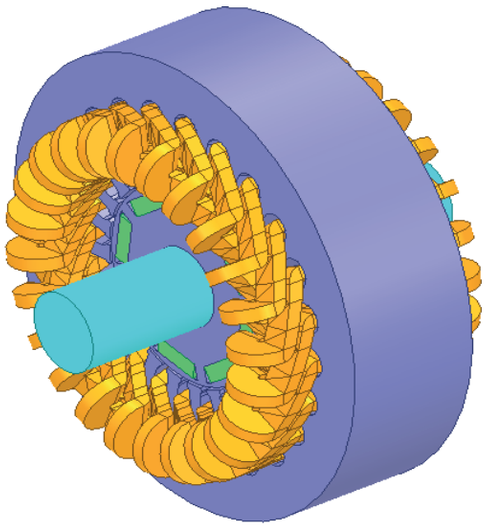

Fig. 3. PMSG geometry.

C. Electromagnetic modeling

In order to have an accurate performance prediction of the PMSG, a detailed electromagnetic model is needed. The three dimensions' electromagnetic model is based on the Laws of Ampere, Faraday, and Gauss (1)-(3). After collecting them, an equation for the magnetic field intensity and the magnetic flux density can be obtained as indicated by (4) which is solved with the FEM [28].

$$\nabla \times \boldsymbol{H} = \sigma_c(\boldsymbol{E}) \tag{1}$$

$$\nabla \times \boldsymbol{E} = -\frac{\partial \boldsymbol{B}}{\partial t} \tag{2}$$

$$\nabla \cdot \boldsymbol{B} = 0 \tag{3}$$

$$\nabla \times \frac{1}{\sigma_c} \nabla \times \boldsymbol{H} + \frac{\partial \boldsymbol{B}}{\partial t} = 0 \tag{4}$$

where the vectors $\boldsymbol{H}$, $\boldsymbol{E}$, and $\boldsymbol{B}$ denote the magnetic field intensity, the electric field, and the magnetic flux density, respectively; the conductivity is indicated by σ_c. A solution of the electromagnetic model is shown in Fig. 4.

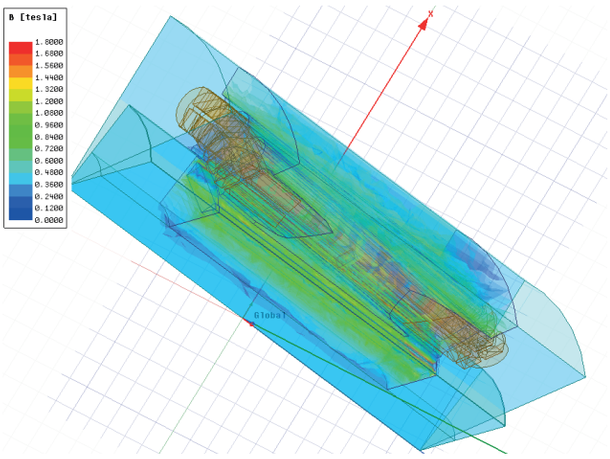

Fig. 4. Magnetic flux density of the PMSG.

D. Surrogate models

Two commonly used heuristic representations are the Response Surface and the Kriging Models. They are also known as surrogate or metamodels. The Surface Response Method (RSM) is made up of a group of statistical techniques used for constructing empirical models [29]. The main objective of RSM is to relate a response, or output variable, η, to the levels of several predictors or input variables, $\xi's$. For example, a surface response can be seen in Fig. 5, which describes the relationship between two input variables, ξ_1 and ξ_2, and an output, η.

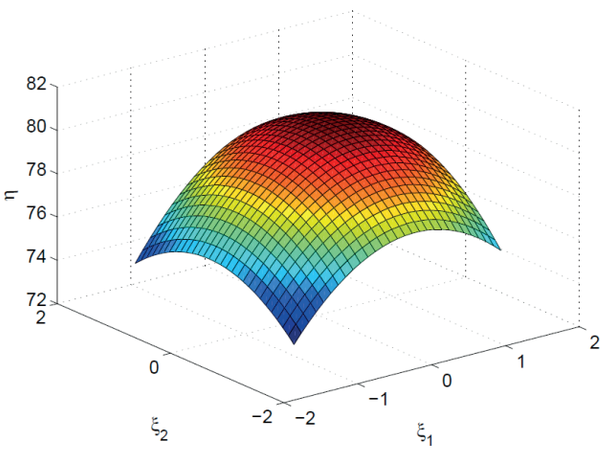

Fig. 5. Response Surface Model with two design variables.

In general, the RSM models have k input variables, $\xi_1, \xi_2, \ldots, \xi_k$, and the relationship between the mean response, η, and the levels, $\xi's$, of the k inputs, can be expressed as:

$$\eta = f(\xi_1, \xi_2, \ldots, \xi_k) \tag{5}$$

In compact form, if ξ denotes a column vector with elements ξ_1, $\xi_2, \ldots, \xi_k$, the mean response function, η, can be written as:

$$\eta = f(\xi) \tag{6}$$

An observed result of the current response is called y. It is said that $y=\eta$, such that the mathematical expectation, $E(y) = \eta$. For this reason, y-η, called the error, ξ, represents the discrepancy between the observed value, y, and the hypothetical mean value, η. In general, the objective is to investigate certain aspects of a functional relationship affected by an error and expressed as:

$$\eta = f(\xi) + \epsilon$$

In practice, it is preferable to employ coded or standardized input variables, x_i, rather than using the natural input variables, ξ_i. There are several coding options, depending on the type of experimental design used. For designs that use coding intervals between 0 and 1, such as factorial designs, (7) is used.

$$x_i = \frac{(\xi_i - \xi_{i0})}{s_i} \tag{7}$$

ξ_{i0} are the centers of the input variables, ξ_i and it is defined as

$$\xi_{i0} = \frac{(\xi_{i\_max} + \xi_{i\_min})}{2}$$

where ξ_{i_max} y ξ_{i_min} are the maximum and minimum limits of the input variables, ξ_i, respectively. The variable S_i represents the distance from the center of the input variables, ξ_i, to their end:

$$S_i = \frac{(\xi_{i\_max} - \xi_{i\_min})}{2}$$

Moreover, designs such as the Central Composite Design use coding intervals between -α and α, and thus (8) can be used.

$$x_i = \begin{cases} -\alpha & \xi_{i\_min} \\ -1 & \frac{(\alpha-1)\xi_{i\_max}+(\alpha+1)\xi_{i\_min}}{2\alpha} \\ 0 & \frac{\xi_{i\_max}+\xi_{i\_min}}{2} \\ +1 & \frac{(\alpha-1)\xi_{i\_min}+(\alpha+1)\xi_{i\_max}}{2\alpha} \\ +\alpha & \xi_{i\_max} \end{cases} \tag{8}$$

In the design of experiments, a polynomial is a function defined by linear combinations of powers and products of coded inputs, $x_1, x_2, \ldots, x_k$. This polynomial is named order d if the higher-order term is d. In RSM, two types of polynomials are commonly used to characterize a phenomenon or process variables: the first-order polynomial and the second-order polynomial, which are defined by (9) and (10), respectively. A first-order polynomial approximation is defined as:

$$y = \beta_0 + \beta_1 x_1 + \beta_2 x_2 + \cdots + \beta_k x_k + \epsilon = \beta_0 + \sum_{i=1}^{k} \beta_i x_i + \epsilon \tag{9}$$

and second-order polynomial approximation as

$$y = \beta_0 + \sum_{i=1}^{k} \beta_1 x_1 + \sum_{i=1}^{k} \beta_{ii} x_i^2 + \cdots + \sum_{i=1}^{k-1} \sum_{j=i+1}^{k} \beta_{ij} x_i x_j + \epsilon \tag{10}$$

where $\beta's$ are the unknown parameters.

On the other hand, the Kriging method has been used for the design of electrical machines. This method also has the advantage of replacing analytical formulations for the design of electrical machines. Some specific analytical models would be impossible to obtain when many design variables are required [30]-[34]. The Kriging method was developed by the South African engineer D.G. Krige in mining applications, where it was used to estimate the amount of gold and other materials. Kriging offers a solution to estimation problems based on a continuous model of stochastic spatial variation. This makes the best use of existing information, taking into account how properties vary in space through a variogram model. In its original formulation, a Kriging estimate at a location was simply a linear or weighted average sum of the data in its neighbourhood. The Kriging method has been developed to solve complex mining, petroleum engineering, pollution control, and public health problems. There are linear and non-linear Kriging. In linear Kriging, the estimates are weighted

linear combinations of data. The weights are assigned to the sampled data in the vicinity of predictions, which minimizes the Kriging estimate of variance [35]. There are several Kriging models such as: ordinary for stationary data, universal for nonstationary data, cokriging for a group of correlated data, etc.

The objective of Kriging is to estimate the values of the random variables, *Z*, at one or more unsampled points, using data sampling as support, that is, $z(x_1), z(x_2), \ldots, z(x_N)$ in the points $x_1, x_2, \ldots, x_N$. The data can be distributed in one, two or three dimensions, although applications in environmental science are usually two-dimensional. Currently, in the design and analysis of electrical machines, data can be distributed in more than three dimensions. Ordinary Kriging is the most common type in practice; it assumes that the mean is unknown. If a point estimate is considered, then *Z* is estimated at a point x_0 as $\hat{Z}(x_0)$, with the same data, and it can be expressed by:

$$\hat{Z}(x_0) = \sum_{i=1}^{N} \lambda_i z(x_i) \tag{11}$$

where λ_i represents the weights.

The expected error is $E\left[\hat{Z}(x_0) - Z(x_0)\right] = 0$

Therefore, the estimated variance can be expressed as:

$$var\left[\hat{Z}(x_0)\right] = E\left[\hat{Z}(x_0) - Z(x_0)\right] = 2\sum_{i=1}^{N} \lambda_i \gamma(x_i, x_0) - \sum_{i=1}^{N}\sum_{j=1}^{N} \lambda_i \lambda_j \gamma(x_i, x_j) \tag{12}$$

where $\gamma(x_i, x_j)$ is the semi-variance of *Z* between x_i and x_j, and $\gamma(x_i, x_0)$ is the semi-variance between point *i* and the target x_0.

There is an associated Kriging variance for each Kriging estimate, denoted by $\sigma^2(x_0)$. The next step in Kriging is to find the weights that minimize these variances, subject to the constraint that their sum must be equal to one, which can be achieved by using the Lagrange multipliers method. In this case, it is defined as an auxiliary function $f(\lambda_i, \psi)$ that contains the variance to be minimized and a term that contains a Lagrange multiplier. Thus the Kriging auxiliary function can be expressed as:

$$T(\lambda_i, \psi) = var\left[\hat{Z}(x_0) - z(x_0)\right] - 2\psi\{\sum_{i=1}^{N} \lambda_i - 1\} \tag{13}$$

Taking the derivatives of (13) with respect to the weights and equating them to zero leads to a set of linear equations with *N+1* unknowns.

$$\sum_{i=1}^{N} \lambda_i \gamma(x_i, x_j) + \psi(x_0) = \gamma(x_j, x_0) \tag{14}$$

$$\sum_{i=1}^{N} \lambda_i = 1 \tag{15}$$

The Kriging equations can be represented as:

$$\boldsymbol{A}\lambda = \boldsymbol{b} \tag{16}$$

where

$$\boldsymbol{A} = \begin{bmatrix} \gamma(x_1, x_1) & \gamma(x_1, x_2) & \cdots & \gamma(x_1, x_N) & 1 \\ \gamma(x_2, x_1) & \gamma(x_2, x_2) & \cdots & \gamma(x_2, x_N) & 1 \\ \vdots & \vdots & \cdots & \vdots & \vdots \\ \gamma(x_N, x_1) & \gamma(x_N, x_2) & \cdots & \gamma(x_N, x_N) & 1 \\ 1 & 1 & \cdots & 1 & 0 \end{bmatrix}$$

$$\lambda = \begin{bmatrix} \lambda_1 \\ \lambda_2 \\ \vdots \\ \lambda_N \\ \psi(x_0) \end{bmatrix}$$

$$\boldsymbol{b} = \begin{bmatrix} \gamma(x_1, x_N) \\ \gamma(x_2, x_0) \\ \vdots \\ \gamma(x_N, x_0) \\ 1 \end{bmatrix}$$

by solving (16), λ can be obtained as:

$$\lambda = \boldsymbol{A}^{-1}\boldsymbol{b} \tag{17}$$

Using direct 3D-FE computations to solve the generator optimization is time-consuming. Therefore, it is common to use heuristical models such as Response Surface Polynomials or Kriging to speed up the design stage in a process. Using Kriging aims to estimate the value of a random function at one or more unsampled points from sparse sample data [35]. To use Kriging is necessary to apply a design of experiments to determine the sampling points and then acquire the information generated by the 3D-FE time-stepping simulations. In this work, the Latin Hypercube sampling was used.

III. Multiobjective Optimization

Many optimizers have been developed over the years, and they are deterministic and stochastic algorithms. Stochastic methods have the property of finding the global optimum. Multiobjective genetic, differential evolution and sequential stage algorithms have been applied to the design of permanent magnet electrical machines [36]-[40]. However, few comprehensive surveys of optimization algorithms used in electrical machine design have been published [41],[42].

Evolutionary algorithms are effective methods for solving optimization problems. The first generation algorithms refer to those that do not include elitism, which is a mechanism for preserving good solutions. A simple implementation would keep a percentage of the best of the current population copying it to the next generation. Then, the standard genetic operations would be applied to create the rest of the new population. There exist different ways in which these algorithms keep the best individuals found during the search process.

The NSGA-II algorithm belongs to second generation algorithms, and it proposed an elitist non-dominated sorting approach, which is used to solve strongly criticized aspects of the previous NSGA algorithm [7],[43]. A parent population P_t of size N is randomly generated and the offspring population Q_t of size N is created from it. Instead of finding the non-dominated front of the offspring population, these two populations are combined into the population R_t of size $2N$. Then a non-dominated sorting is applied to the resultant population R_t and all members are classified. This is done to perform a global non-domination check among the offspring and parent solution, resulting in a new population filled by solutions of different non-dominated fronts. The filling begins with the best non-dominated front followed by the second non-dominated front, and so on, one at a time. Since the overall population size is $2N$ and there are only N slots available, not all fronts can be accommodated, and they are just deleted. The NSGA-II procedure is outlined below.

1. Combine parent and offspring population and create $R_t = P_t \cup Q_t$.

   Perform a non-dominated sorting to $R_t$and identify fronts: $F_i, i = 1, 2, ...,$ etc.
2. Set new population P_{t+1} $P_{t+1} = \emptyset$. Set a counter $i = 1$.

   Until $|P_{t+1}| + |F_i| < N$, perform $P_{t+1} = P_{t+1} \cup F_i$ and $i = i + 1$.
3. Perform the crowding-sort ($F_i \prec_c$) procedure and include the most widely spread $(N - |P_{t+1}|)$ solutions by using the crowding distance values in the sorted F_i to P_{t+1}.
4. Create offspring population $Q_{t+1}$from P_{t+1} by using the crowded tournament selection, crossover and mutation operators.

In step 3, the crowding-sorting of the solutions of front (the last front which could not be accommodated fully) is performing by using a *crowding distance metric*. The population is arranged in descending order of magnitude of the crowding distance values. In step 4, a crowding tournament selection operator, which also uses the crowding distance, is used. The non-dominated sorting in step 1 and filling up population P_{t+1} can be performed together.
The crowded-comparison operator ($\prec_c$) guides the selection process at the various stages of the algorithm toward a uniformly spread-out Pareto-optimal front. Assume that every individual i in the population has two attributes:

1. Nondominant rank (i_{rank})
2. Crowding distance ($i_{distance}$)

A partial order $\prec_c$ is defined as:
$i \prec_c j$ if($i_{rank} < j_{rank}$)
or ((i_{rank}=j_{rank}) and ($i_{distance}$>$j_{distance}$))

There is a so-called niching strategy that refers to choosing members of the last front instead of just discarding them. This kind of strategy affects the algorithm in the latter simulation stages but not very much in the early stages of evolution.
The computational complexity of the NSGA-II non-dominated sorting approach is $O(mN^2)$, where m refers to the number of objectives an N stands for the population size. In NSGA-II applied to solve a 2 objective DTLZ1 with a population size of 1000 and a maximum generation of 500, non-dominated sorting consumes more than 70% of its runtime [44]. The computational cost increases if the population size and/or the number of objectives are also increased. NSGA-III appears as an extension of NSGA-II to improve its performance in many-objective problems [45]. NSGA-III has the same general procedures as NSGA-II, but it differs in the selection process used to create a new population based on reference points.

IV. PMSG DESIGN SIMULATION RESULTS

Thorough statistical analysis the correlation between the input variables and the output functions is determined (Table I). The correlations are computed using the Spearman algorithm because it can be used for linear and nonlinear relationships between variables [27]. In this research work, 14 design variables were taken into account; five of them were associated with the slot dimensions. The axial length of the generator, airgap, skew, rotor diameter, and length of the stator yoke were also selected. The generated output power and the total generator weight are the two output functions. In Fig. 6, the correlations in red and blue are shown, where the ones out of the diagonal have a more strong participation in the objective functions. It can be seen that five variables have the highest impact: the axial length of the generator, the rotor diameter, the length of the stator yoke, the airgap, and the height of the stator slot. A positive value indicates an increment in the dependent variable due to an increase in the independent variable. A negative value indicates a decrease in the output function due to an increase in the input variables. The sensitivities of these five design variables are shown in Table II.

TABLE I
DESIGN VARIABLES AND OUTPUT FUNCTIONS

Name	Definition	Name	Definition
P_1	Axial length	P_9	Rotor diameter
P_2	Airgap	P_{10}	PM bridge
P_3	Skew	P_{11}	PM rib
P_4	Slot bottom height	P_{12}	PM width
P_5	Slot height	P_{13}	PM thickness
P_6	Slot opening	P_{14}	Stator yoke length
P_7	Slot lower width	P_{15}	Output power
P_8	Slot upper width	P_{16}	Generator weight

TABLE II
SENSITIVITIES OF THE SELECTED DESIGN VARIABLES

Design variable	Output power (%)	Generator weight (%)
Airgap	-6.41	0.83
Stator yoke length	-0.48	39.81
Axial length	5.05	9.15
Slot height	0.18	29.36
Rotor diameter	-84.63	20.79

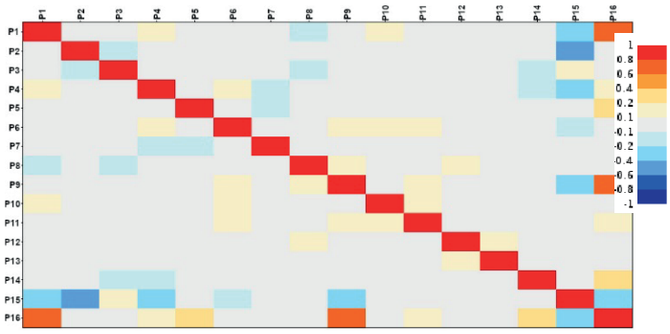

Fig. 6. Correlation matrix of the design variables and objective functions.

The optimization problem is defined by minimization of the total generator weight. Minimizing the weight means minimizing the quantity of the materials used, which also lower the costs. The generator must also supply the specified electric power. Thus, the objective functions are the output power and the generator's weight, which depend on the design variables which are constrained by lower and upper bounds. In the case of the generator, its total weight is a function of the core of the stator and rotor, which is made of non-oriented magnetic laminations, the weight of copper conductors, the weight of the permanent magnets, and the shaft weight.

On the other hand, the output power is calculated as the product of the voltages and currents. The design specification of the PMSG generator consists of a 900 W generator, a speed of 900

rpm, a voltage of 220 V, and a three-phase wye connection. The optimization problem can be expressed as in (18)-(20).

$$\min \{P_{out}, W_{gen}\} \tag{18}$$

s.t.

$$P_{out} = P_{rated}$$

$$\boldsymbol{x}_l \leq \boldsymbol{x} \leq \boldsymbol{x}_u$$

where:

$$W_{gen} = W_{core} + W_{cu} + W_{pm} + W_{shaft} \tag{19}$$

$$P_{out} = v_a i_a + v_b i_b + v_c i_c \tag{20}$$

In the above equations, $\boldsymbol{x}$ is a design variable vector whose elements are indicated in Table II. The subscripts l and u indicate lower and upper bounds, respectively. P_{out} and P_{rated} represent the generated and rated machine electrical powers of the PMSG. W denotes weight and subscripts *gen*, *core*, *cu*, *pm,* and *shaft* stand for generator, stator and rotor core, copper of windings, permanent magnets, and steel shaft, respectively. Voltages and currents of PMSG phases *a*,*b*,*c* are indicated by v and i, respectively.

The optimization problem described by (18)-(20) was solved using the evolutionary non-sorting multiobjective algorithm [7]. The numerical results obtained with the Kriging model for the output power and weight cost functions are presented in the following figures. The two cost functions are plotted against the design variables and only those with significant variations on the cost function are illustrated, those with more significant variations corresponds with the sensitivity results shown in Table II. However, each objective is a function of the five design variables The generator power as a function of the airgap and axial length is shown in Fig. 7, where it can be clearly seen that the Kriging model shows a slight variation when airgap is varied by approximately 1mm and the axial length by 4mm. The flatness seen in the surface is due to the opposite sign in the sensitivities of airgap and axial length with respect to the active electrical power. Whereas in Fig. 8, the output electrical power is plotted as a function of the axial length and rotor diameter, significant variations in power is seen as it is expected due to the change in electromagnetic torque due to the variation of the rotor diameter. The PMSG is being operated at a constant speed. Besides, the sensitivity of the rotor diameter, shown in Table III, has a value of -84.6%, it means that a considerable variation in the objective of output power must be obtained, as it is correctly shown in Fig. 8. Significant variations are also seen in the cost function of electrical power when plotted against the axial length and the rotor diameter as illustrated in Fig. 9, due to the significant correlation and sensitivity that exists between output power and rotor diameter. The output power variation of the PMSG versus airgap and stator slot height is seen in Fig. 10. Finally, the plot of the active power against airgap and stator yoke length is seen in Fig. 11, where the airgap has a larger sensitivity and both of them have negative values as indicated in Table III. The generator's weight as a function of the axial length and rotor diameter is illustrated in Fig. 12. Both design variables have positive sensitivity values as seen in Table III and is also indicated by the slope plane. The plot of the PMSG weight objective as a function of the airgap and stator slot height is illustrated in Fig. 13. The plots of the PMSG weight function have similar surfaces. Finally, the optimized solutions are represented by the Pareto front of the two cost functions, this can been seen in Fig. 14, where the active power and weight are plotted. A selected candidate solution is shown in Table III, and it has a calculated efficiency of 96%.

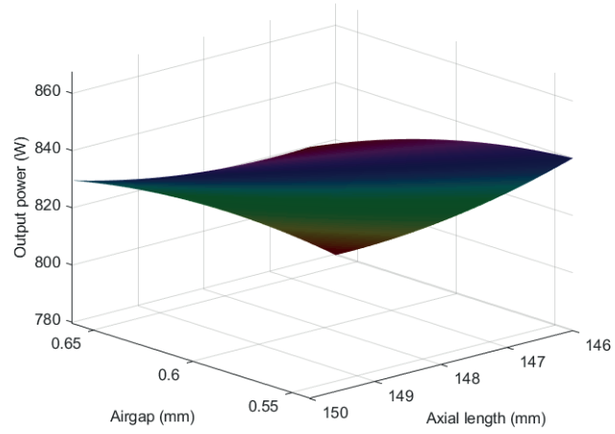

Fig. 7. Generated power as a function of the airgap and axial length.

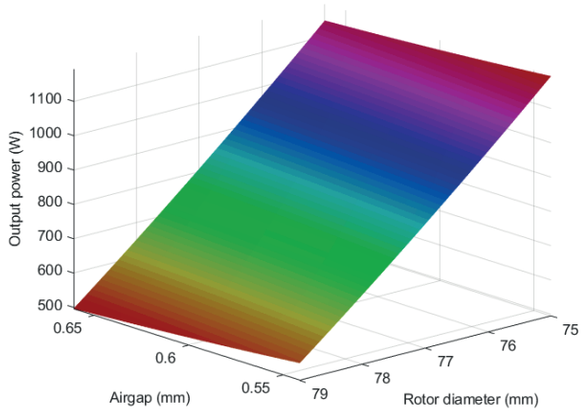

Fig. 8. Generated power as a function of the airgap and rotor diameter.

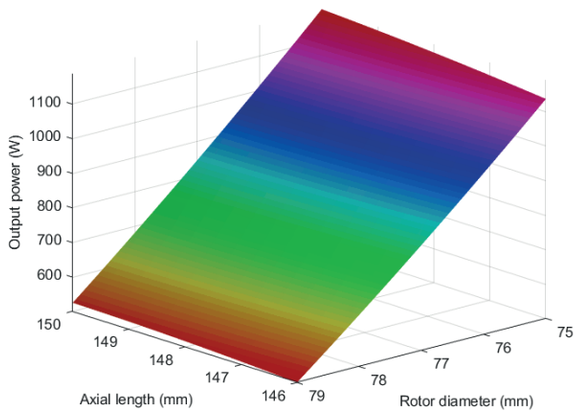

Fig. 9. Output electrical power as a function of the axial length and rotor diameter.

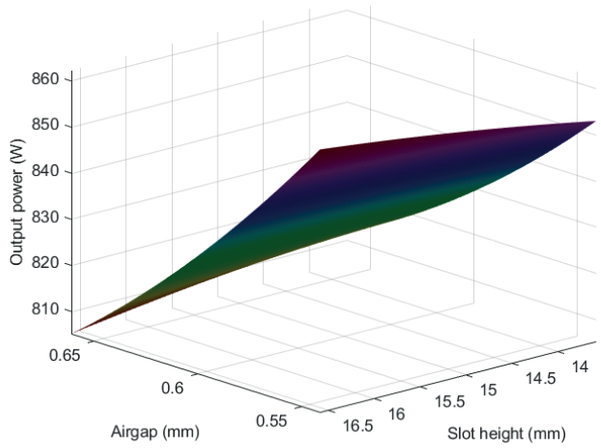

Fig. 10. Generated power as a function of the airgap and stator slot height.

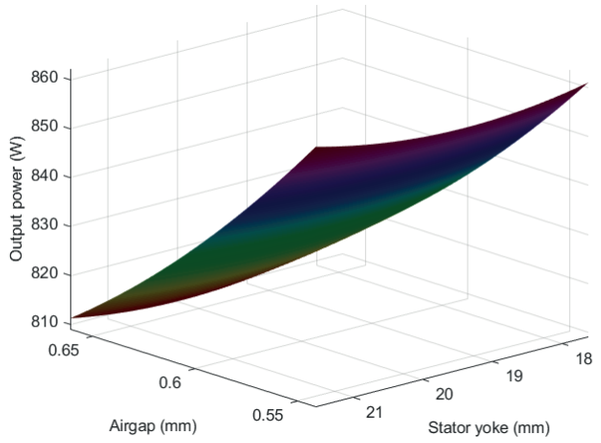

Fig. 11. Generated power as a function of the airgap and stator yoke length.

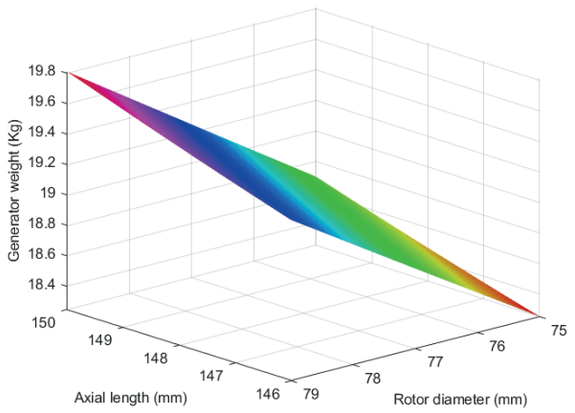

Fig. 12. Generator weight as a function of the axial length and rotor diameter.

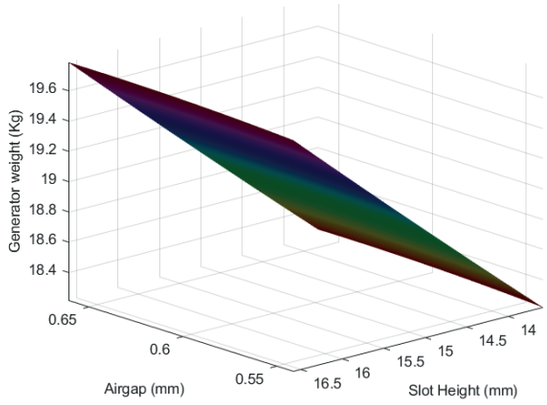

Fig. 13. Generator weight as a function of the airgap and stator slot height.

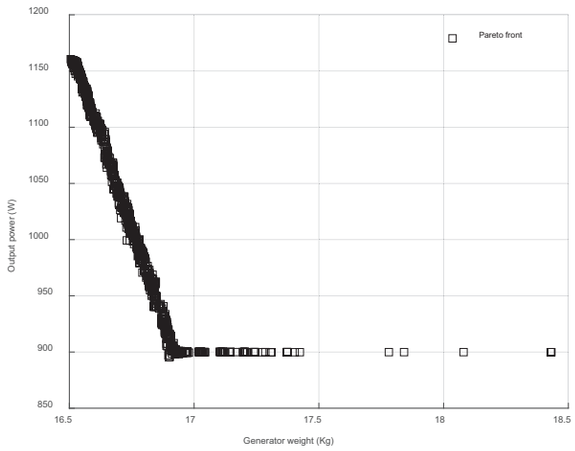

Fig. 14. Pareto front obtained by solving the multiobjective optimization problem.

TABLE III
CANDIDATE OPTIMUM SOLUTION

Design variable	Value
Airgap	0.6202 mm
Axial length	17.649 mm
Rotor diameter	146.71 mm
Stator yoke length	13.655 mm
Stator slot height	76.424 mm
Output power	900.33 W
Generator weight	17.02 Kg

V. CONCLUSION

This article has presented an optimal design of a PMSG using a multiobjective genetic algorithm and Kriging metamodeling. It is important to have a reduced design space in the design of electrical machines, where there are many design variables. Therefore, it allows less 3D-FE PMSG number of simulation operating points in the design of experiments. Hence, the construction of the surrogate model is faster. Furthermore, applying correlation and sensitivity analysis allows engineers to speed up the electrical machine design because the analysis allows finding a reduced set of design variables. Otherwise, only an expert on generator design has the knowledge acquired by years of experience.

VI. References

[1] Bu, J., Zhou, M., Lan, X., and Lv, K., "Optimization for Airgap Flux Density Waveform of Flywheel Motor Using NSGA-2 and Kriging Model Based on MaxPro Design," *IEEE Trans. Magn*., 53(8), 2017, pp. 1–7.

[2] Pyrhönen, J., Jokinen, T., and Hrabovcová, V., 2013, *Design of Rotating Electrical Machines*.

[3] Kim, J. B., Hwang, K. Y., and Kwon, B. I., "Optimization of Two-Phase in-Wheel IPMSM for Wide Speed Range by Using the Kriging Model Based on Latin Hypercube Sampling," *IEEE Trans. Magn*., 47(5), 2011, pp. 1078–1081.

[4] Park, H. J., Yeo, H. K., Jung, S. Y., Chung, T. K., Ro, J. S., and Jung, H. K., "A Robust Multimodal Optimization Algorithm Based on a Sub-Division Surrogate Model and an Improved Sampling Method," *IEEE Trans. Magn*., 54(3), 2018, pp. 2018–2021.

[5] Ren, Z., Ma, J., Qi, Y., Zhang, D., and Koh, C.-S., "Managing Uncertainties of Permanent Magnet Synchronous Machine by Adaptive Kriging Assisted Weight Index Monte Carlo Simulation Method," *IEEE Trans. Energy Convers.*, 35(4), 2020, pp. 2162–2169.

[6] Arjona, M. A., Hernandez, C., and Cisneros-Gonzalez, M., "Hybrid Optimum Design of a Distribution Transformer Based on 2-D FE and a Manufacturer Design Methodology," *IEEE Trans. Magn*., 46(8), 2010, pp. 2864–2867.

[7] Kalyanmoy Deb, *Multi-Objective Optimization Using Evolutionary Algorithms*, John Wiley & Sons, Ltd. 2001.

[8] Xuerong, Y., Hao, C., Huimin, L., Xinjun, C., and Jiaxin, Y., "Multi-Objective Optimization Design for Electromagnetic Devices With Permanent Magnet Based on Approximation Model and Distributed Cooperative Particle Swarm Optimization Algorithm," *IEEE Trans. Magn.*, 54(3), 2018, pp. 1–5.

[9] Shin, D. J., and Kwon, B. Il, "Multi-Objective Optimal Design for in-Wheel Permanent Magnet Synchronous Motor," *Proc. - 12th Int. Conf. Electr. Mach. Syst. ICEMS 2009*, 45(3), 2009, pp. 1780–1783.

[10] Padmanathan, K., Kamalakannan, N., Sanjeevikumar, P., Blaabjerg, F., Holm-Nielsen, J. B., Uma, G., Arul, R., Rajesh, R., Srinivasan, A., and Baskaran, J., "Conceptual Framework of Antecedents to Trends on Permanent Magnet Synchronous Generators for Wind Energy Conversion Systems," *Energies*, 12(13), 2019.

[11] Li, M., Gabriel, F., Alkadri, M., and Lowther, D. A., "Kriging-Assisted Multi-Objective Design of Permanent Magnet Motor for Position Sensorless Control," IEEE Trans. Magn., 52(3), 2016, pp. 17–20.

[12] Dhiman, G., and Kumar, V., "Emperor Penguin Optimizer: A Bio-Inspired Algorithm for Engineering Problems," *Knowledge-Based Syst*., 159(6), 2018, pp. 20–50.

[13] Niu, Q., Zhang, L., and Li, K., "A Biogeography-Based Optimization Algorithm with Mutation Strategies for Model Parameter Estimation of Solar and Fuel Cells," *Energy Convers. Manag*., 86, 2014, pp. 1173–1185.

[14] Baek, S. W., and Lee, S. W., "Design Optimization and Experimental Verification of Permanent Magnet Synchronous Motor Used in Electric Compressors in Electric Vehicles," *Appl. Sci*., 10(9), 2020.

[15] Li, L., Li, W., Li, D., Li, J., and Fan, Y., "Research on Strategies and Methods Suppressing Permanent Magnet Demagnetization in Permanent Magnet Synchronous Motors Based on a Multi-Physical Field and Rotor Multi-Topology Structure," *Energies*, 11(1), 2018.

[16] Jung, J. W., Lee, B. H., Kim, K. S., and Kim, S. Il, "Interior Permanent Magnet Synchronous Motor Design for Eddy Current Loss Reduction in Permanent Magnets to Prevent Irreversible Demagnetization," *Energies*, 13(19), 2020.

[17] Dong, F., Zhao, J., Song, J., Feng, Y., and He, Z., "Optimal Design of Permanent Magnet Linear Synchronous Motors at Multispeed Based on Particle Swarm Optimization Combined with Sn Ratio Method," *IEEE Trans. Energy Convers*., 33(4), 2018, pp. 1943–1954.

[18] Hu, P., and Wang, D., "Analytical Average Torque Optimization Method of Parallel Magnetized Surface-Mounted Permanent-Magnet Machine with Third-Order Harmonic Shaping Method," *IEEJ Trans. Electr. Electron. Eng.*, 15(9), 2020, pp. 1377–1383.

[19] Wang, Q., Zhao, P., Du, X., Lin, F., and Li, X., "Electromagnetic Vibration Analysis and Slot-Pole Structural Optimization for a Novel Integrated Permanent Magnet in-Wheel Motor," *Energies*, 13(13), 2020.

[20] Guyadec, M. Le, Gerbaud, L., Vinot, E., Reinbold, V., and Dumont, C., "Use of Reluctance Network Modelling and Software Component to Study the Influence of Electrical Machine Pole Number on Hybrid Electric Vehicle Global Optimization," *Math. Comput. Simul*., 158, 2019, pp. 79–90.

[21] Fang, S., Xue, S., Pan, Z., Yang, H., and Lin, H., "Torque Ripple Optimization of a Novel Cylindrical Arc Permanent Magnet Synchronous Motor Used in a Large Telescope," *Energies*, 12(3), 2019.

[22] Liang, J., Parsapour, A., Yang, Z., Caicedo-Narvaez, C., Moallem, M., and Fahimi, B., "Optimization of Air-Gap Profile in Interior Permanent-Magnet Synchronous Motors for Torque Ripple Mitigation," *IEEE Trans. Transp. Electrif.*, 5(1), 2019, pp. 118–125.

[23] Carraro, E., Bianchi, N., Zhang, S., and Koch, M., "Design and Performance Comparison of Fractional Slot Concentrated Winding Spoke Type Synchronous Motors with Different Slot-Pole Combinations," *IEEE Trans. Ind. Appl*., 54(3), 2018, pp. 2276–2284.

[24] Onsal, M., Cumhur, B., Demir, Y., Yolacan, E., and Aydin, M., "Rotor Design Optimization of a New Flux-Assisted Consequent Pole Spoke-Type Permanent Magnet Torque Motor for Low-Speed Applications," IEEE Trans. Magn., 54(11), 2018.

[25] Bjørk, R., Bahl, C. R. H., and Insinga, A. R., "Topology Optimized Permanent Magnet Systems," *J. Magn. Magn. Mater*., 437, pp. 78–85, 2017.

[26] Li, Y., Chai, F., Song, Z., and Li, Z., "Analysis of Vibrations in Interior Permanent Magnet Synchronous Motors Considering Air-Gap Deformation," *Energies*, 10(9), 2017.

[27] Walpole, R. E., Myers, R. H., Myers, S. L., and Ye, K.,, *Probability & Statistics for Engineers & Scientists 9th Ed*. 2011.

[28] ANSYS, 2020, "Maxwell User Manual."

[29] Myers, R. H., Montgomery, D. C., and Anderson-cook, C. M., *Response Surface Methodology 3rd Edition*. 2009.

[30] Lebensztajn, L., RondiniMarretto, C. A., CaldoraCosta, M., and Coulomb, J.-L., "Kriging: A Useful Tool for Electromagnetic Device Optimization," *IEEE Trans. Magn.*, 40(2), 2004, pp. 1196–1199.

[31] Kim, J. B., Hwang, K. Y., and Kwon, B. I.,

"Optimization of Two-Phase In-Wheel IPMSM for Wide Speed Range by Using the Kriging Model Based on Latin Hypercube Sampling," *IEEE Trans. Magn.*, 47(5), 2011, 2011, pp. 1078–1081.

[32] Zhang, Y., Xia, B., Xie, D., and Koh, C. S., "Optimum Design of Switched Reluctance Motor to Minimize Torque Ripple Using Ordinary Kriging Model and Genetic Algorithm," *2011 International Conference on Electrical Machines and Systems*, *IEEE*, 2011, pp. 1–4.

[33] Zhang, Y., Jingguo Yuan, Xie, D., In Sung Hwang, and Koh, C. S., "Shape Optimization of a PMLSM Using Kriging and Genetic Algorithm," *2010 5th IEEE Conference on Industrial Electronics and Applications*, IEEE, 2010, pp. 1496–1499.

[34] Bilicz, S., Lambert, M., Gyimothy, S., and Pavo, J., "Solution of Inverse Problems in Nondestructive Testing by a Kriging-Based Surrogate Model," *IEEE Trans. Magn.*, 48(2), 2012, pp. 495–498.

[35] Webster, R., and Oliver, M. A., *Geostatistics for Environmental Scientists: Second Edition*. 2008.

[36] Cavagnino, A., Bramerdorfer, G., and Tapia, J. A., "Optimization of Electric Machine Designs−Part I," *IEEE Trans. Ind. Electron.*, 64(12), 2017, pp. 9716–9720.

[37] Cavagnino, A., Bramerdorfer, G., and Tapia, J. A., "Optimization of Electric Machine Designs - Part II," *IEEE Trans. Ind. Electron.*, 65(2), 2018, pp. 1700–1703.

[38] Edhah, S. O., Alsawalhi, J. Y., and Al-Durra, A. A., "Multi-Objective Optimization Design of Fractional Slot Concentrated Winding Permanent Magnet Synchronous Machines," *IEEE Access*, **7**, 2019, pp. 162874–162882.

[39] Tong, W., Wei, H., Li, S., and Zheng, J., "A Novel Multi-objective Optimization Method for the Optimization of Interior Permanent Magnet Synchronous Machines," *IET Electr. Power Appl.*, 15(3), 2021, pp. 359–369.

[40] Lei, G., Bramerdorfer, G., Ma, B., Guo, Y., and Zhu, J., "Robust Design Optimization of Electrical Machines: Multi-Objective Approach," *IEEE Trans. Energy Convers.*, 36(1), 2021, pp. 390–401.

[41] Lei, G., Zhu, J., Guo, Y., Liu, C., and Ma, B., "A Review of Design Optimization Methods for Electrical Machines," *Energies*, 10(12), 2017, p. 1962.

[42] Dineva, A., Mosavi, A., Faizollahzadeh Ardabili, S., Vajda, I., Shamshirband, S., Rabczuk, T., and Chau, K.-W., "Review of Soft Computing Models in Design and Control of Rotating Electrical Machines," *Energies,* **12**(6), 2019, p. 1049.

[43] Deb, K., Pratap, A., Agarwal, S., and Meyarivan, T., "A Fast and Elitist Multiobjective Genetic Algorithm: NSGA-II," *IEEE Trans. Evol. Comput.*, 6(2), 2002, pp. 182–197.

[44] Tian, Y., Wang, H., Zhang, X., and Jin, Y., "Effectiveness and Efficiency of Non-Dominated Sorting for Evolutionary Multi- and Many-Objective Optimization," *Complex Intell. Syst.*, 3(4), 2017, pp. 247–263.

[45] Deb, K., and Jain, H., "An Evolutionary Many-Objective Optimization Algorithm Using Reference-Point-Based Nondominated Sorting Approach, Part I: Solving Problems with Box Constraints," *IEEE Trans. Evol. Comput.*, 18(4), 2014, pp. 577–601.

AUTHORS NAME AND AFFILIATION

Marco Arjona, Concepcion Hernandez, Jorge Lara
Research and Graduate Department
Electrical Power and Renewable Energy Research Group.
La Laguna Institute of Technology (TecNM).
27000 Torreon, Coahuila. Mexico.
+52 871 1264780, marjona@ieee.org